Journal of
Nano Systems & Technology

October, 2009 |www.jnst.org

JNST.2009.001

Fabrication and Multifunctional Properties of High Volume Fraction Aligned Carbon Nanotube Thermoset Composites

Enrique J. Garcia[1], Diego S. Saito[2], Ludovico Megalini[3],
A. John Hart[4], and Roberto Guzman de Villoria[5], and Brian L. Wardle[6]
Massachusetts Institute of Technology, Cambridge, MA, 02139

ABSTRACT

High volume fraction aligned carbon nanotube (CNT) nanocomposite specimens are fabricated using mechanical densification of CNT forests and capillarity-induced wetting of the forests with several thermoset polymers. Such nanocomposites approach the ideal morphology of collimated aligned fiber systems used in aerospace composites, and have long been expected to exhibit substantial engineering property improvements over existing systems. Polymers used are unmodified and include two aerospace-grade complex thermosets and a UV-curing thermoset used in microfabrication. Mechanical densification of the CNT forests prior to polymer introduction results in uniform nanocomposites. High volume fraction (to ~20%) CNT forests are effectively wet by the thermosets studied. Modulus, hardness, and electrical resistivity are characterized as a function of volume fraction for one of the epoxy systems. Multifunctional properties (modulus, hardness, and electrical conductivity) of the nanocomposites are strongly influenced by CNT volume fraction. Such specimens can be used to explore nano-scale interaction effects such as CNT-CNT contact effects on thermal and electrical conductivities.

Nomenclature

E	=	Young´s modulus of sample in nanoindentation
E_i	=	Young´s modulus of indenter in nanoindentation
E_r	=	Reduced modulus in nanoindentation
H	=	Hardness
V_f	=	Volume fraction
ρ	=	Resistivity
ν	=	Poisson's ratio of sample in nanoindentation
ν_i	=	Poisson's ratio of indenter in nanoindentation

I. Introduction

ADVANCED composites utilizing aligned carbon nanotubes (CNTs) in various morphologies are being developed targeting enhanced laminate-level multifunctional properties. Since their identification [1,2], CNTs have been envisioned as a constituent in various applications due to their numerous and attractive multifunctional

[1] Postdoctoral Associate, Department of Aeronautics and Astronautics, MIT. Currently Chief Engineer, Gamesa Innovation and Technology, Sarriguren (Spain).
[2] Visiting Student (Instituto Tecnologico de Aeronautica, Brazil), Department of Aeronautics and Astronautics.
[3] Visiting Student (Politecnico di Torino, Italy – INP Grenoble, France – EPF Lausanne, Switzerland), Department of Aeronautics & Astronautics.
[4] Postdoctoral Associate, Department of Aeronautics and Astronautics. Currently Assistant Prof., Dept. of Mech. Eng., University of Michigan.
[5] Postdoctoral Associate, Department of Aeronautics and Astronautics, MIT 41-317, 77 Massachusetts Ave., Cambridge, MA, 02139 (USA).
[6] Associate Professor, Department of Aeronautics and Astronautics, MIT 33-314, 77 Massachusetts Ave., Cambridge, MA, 02139 (USA). *Corresponding author:* wardle@mit.edu

(*i.e.,* mechanical and nonmechanical) properties. At small scales, and for defect-free CNTs, many of their mechanical properties are unrivaled by any other material, especially when the properties are normalized to density, (*e.g.,* specific stiffness, modulus over density, E/ρ), making them an attractive material for aerospace applications. The most common approach to realize the attractive properties of CNTs is the combination of CNTs and polymers to create polymer nanocomposites (PNCs). However, it has proven difficult to produce nanocomposites that take full advantage of CNT properties at engineering-relevant length scales due to synthesis/fabrication issues. Hybrid systems, or 'nano-engineered composites', employing aligned-CNTs arranged within existing advanced fibers and matrices have been developed (see Figure 1) [3-5]. In this case, the aligned-CNT polymeric nanocomposite is part of a larger microstructural description of the hybrid nano-engineered composite laminate. The representative volume element (RVE) shown in Figure 1 is the subject of this paper, and it is studied experimentally as a function of aligned-CNT volume fraction.

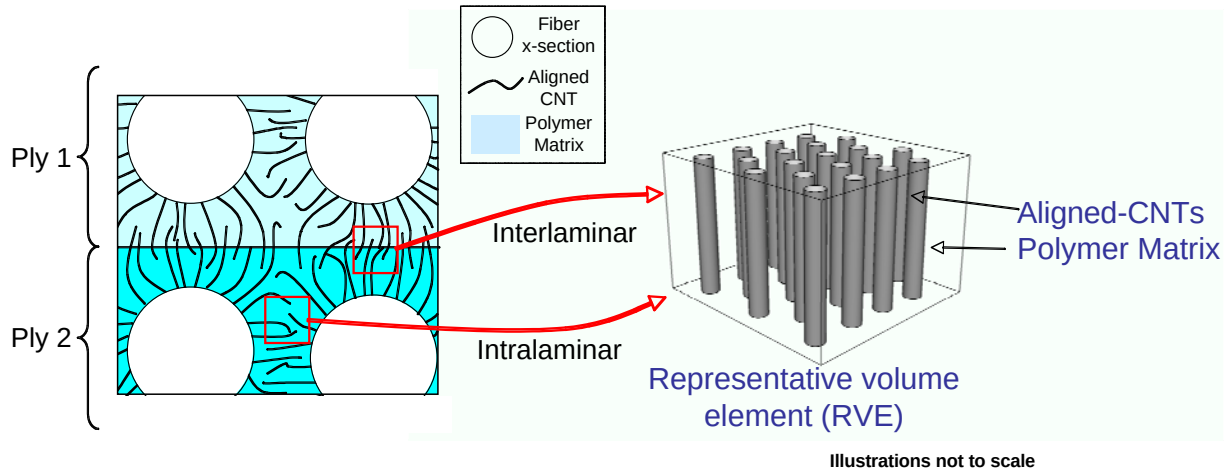

Figure 1. Illustration of aligned-CNTs in a nano-engineered composite indicating the representative volume element (RVE) of an aligned-CNT PNC [0-0]. CNT alignment and spacing in the RVE are idealized.

Similar to existing advanced composites, the *ideal* PNC has high volume fraction (V_f) of aligned, continuous, high-quality CNTs homogeneously dispersed in a surrounding matrix with no voids *(i.e.,* the composite is simply aligned-CNTs and matrix). In advanced composite materials (*e.g.*, carbon fiber reinforced plastics, CFRP), high fiber volume fraction allows the properties of the advanced fibers to dominate the composite properties, while the matrix provides support (*e.g.*, from buckling under shear or compression), protection, and a path for load-sharing between the fibers. The ideal nanocomposite morphology likely looks similar, with the CNTs replacing the micron-diameter fibers as the reinforcement. The effect of CNT alignment on nanocomposite mechanical properties is significant (220% vs. <100%) [6]. Typical V_f's for CNTs dispersed in polymers are only a few % and dispersion of the CNTs is difficult to achieve [7-8]. In this paper, we discuss a densification platform that allows the production of high volume fraction aligned-CNT/polymer nanocomposites by mechanical densification of forests of aligned-CNTs. Our process allows mm-scale specimens of near-ideal morphology nanocomposites to be fabricated: aligned-CNT PNCs with ultra-high (approaching practical and theoretical limits) CNT volume fraction (to ~20%). The examples in Figure 2 show various volume fractions of aligned-CNT forests before wetting with a polymer, and the example in Figure 3 shows ideal morphology nanocomposites. Using the densification platform, variable-V_f CNT/polymer nanocomposite specimens are fabricated and subjected to multifunctional characterizations. Results of the fabrication studies, as well as the multifunctional testing of PNCs with the ideal morphology are discussed.

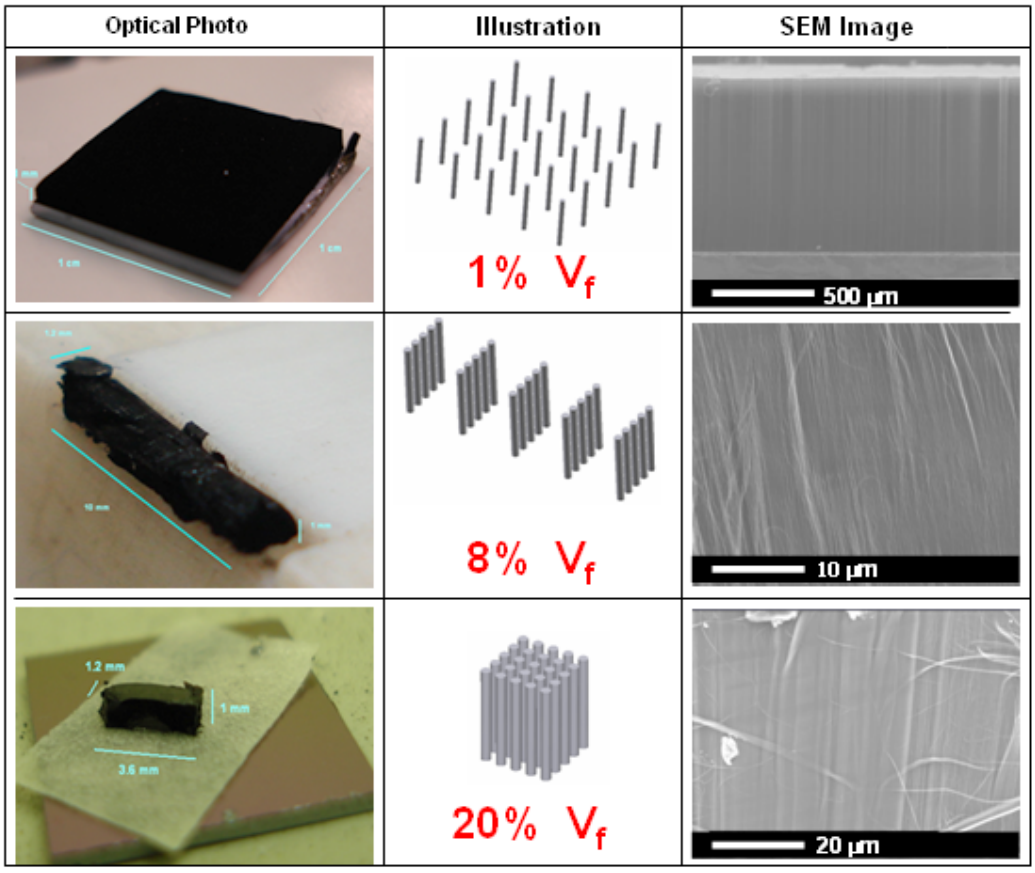

Figure 2. Collage illustrating mechanical densification of aligned-CNT forests for subsequent wetting by polymers to form aligned-CNT PNCs. A 1 cm^2 as-grown CNT forest at 1% V_f is shown in the first row. Scale bars are 500 μm, 10 μm, and 20 μm, respectively.

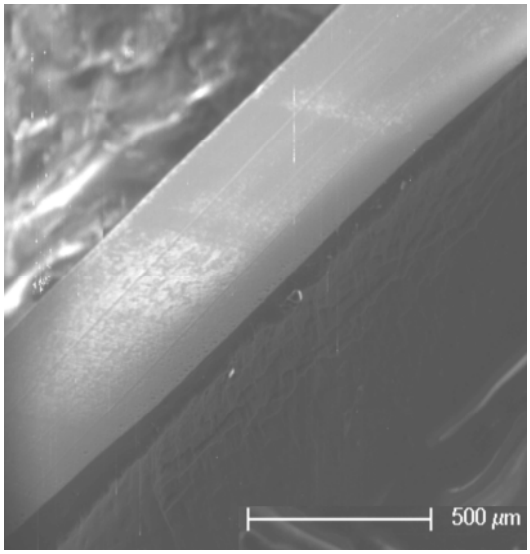

Figure 3. Ideal morphology nancomposite with aerospace-grade thermoset (VRM34) polymer matrix: SEM of a high (22%) V_f NC after machining. Scale bar is 500 μm.

II. Experimental Methods

In this section, the procedures and details of materials are provided, focusing on aligned-CNT PNC fabrication and characterization by mechanical and electrical testing.

A. Aligned-CNT Polymer Nanocomposite Fabrication

Fabrication of aligned-CNT PNCs relies on a simple overall process: (1) Multi-walled CNTs (MWCNTs) of ~8nm diameter are grown using chemical vapor deposition and processes developed at MIT [9,10] using an alumina/Fe catalyst system and ethylene carbon source. Self-aligned-CNT forests of ~1% volume fraction (~80 nm spacing between CNTs) are grown at atmospheric pressure at rates exceeding 2 μm/s to heights between 0.5 and 1 mm for this study. (2) The CNT forest is then delaminated using mechanical means (a laboratory razor blade) to achieve a freestanding aligned-CNT film. The CNT forests/films are coherent structures that have finite stiffness due to the self-aligned-CNT entanglement during growth. (3) Biaxial mechanical densification is used to densify the as-grown forests and allows volume fraction to be controlled from 1-20%. (4) The CNT forest is placed on a z-stage using SEM tape and immersed in a pool of polymer at the temperatures indicated in Table 1. The polymers are drawn up into the aligned-CNT forest via capillary action [11], a strong mechanism noted in earlier work to fabricate micron-scale nanocomposites for compression testing [6]. (5) The polymer-impregnated CNT forest is removed from the z-stage, cured as given in Table 1, and then diesawed prior to inspection via optical and scanning-electron microscopy. The overall process for fabrication and inspection is provided in Figure 4, and polymers studied are shown in Table 1.

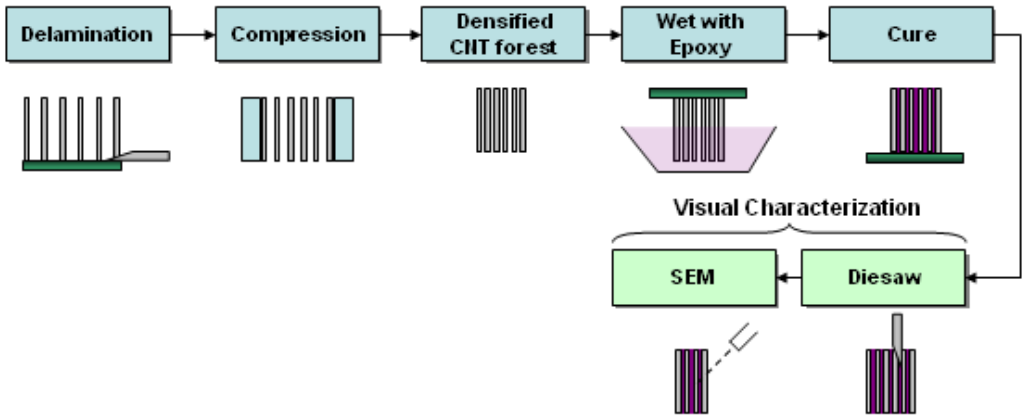

Figure 4. Overall process for fabricating aligned-CNT polymer nanocomposites (PNCs).

Table 1. Properties of epoxies used in this study.

Epoxy	Supplier	Typical Application	Epoxy Temperature for Wetting	Viscosity at Wetting Temp.	Cure Cycle
VRM34	Hexcel	Aerospace Composite	90°C	12 cP	1 hour under 160° C 3 hours under 180° C
RTM6	Hexcel	Aerospace Composite	90°C	33 cP	1 hour under 160° C 3 hours under 180° C
SU-8 2002	MicroChem	Microfabrication	65° C	8 cP	Pre-bake: 60°C for 5 min UV light exposure for 1 min Pos-Bake: 90°C for 5 min Hard bake: 130°C for 30 min
SU-8 2010	MicroChem	Microfabrication	65° C	450 cP	Same as SU-8 2002
SU-8 2015	MicroChem	Microfabrication	65° C	1500 cP	Same as SU-8 2002
SU-8 2025	Microchem	Microfabrication	65° C	2300 cP	Same as SU-8 2002

Note that two nanoscale particle exposure studies [12, 13] have been completed related to working with the aligned-CNT forests and composites handled in the manner described herein.

B. Characterization

The aligned-CNT PNC morphology is evaluated using optical and scanning-electron microscopy (SEM). SEM predominately utilizes a JEOL 5910 and also a Philips XL 30, having resolutions of 1 μm and 50 nm, respectively. Volume fraction for all samples is assessed by volumetric considerations. As-grown forests have an aligned-CNT V_f of 1%, and after biaxial densification, sample size is used to calculate the new V_f.

C. Nanoindentation

Modulus and hardness of the PNCs along the CNT axis were inferred using standard nanoindentation testing. Samples were prepared as described above, and the surface was polished with progressively finer sandpaper to a roughness of less than 0.3 μm (determined by SEM). The tests were performed using a Nanotest 600 nanomechanical testing system (Micro Materials, UK) [14]. The nanoindenter monitors and records the load and displacement of the indenter with a force resolution of ~100 nN and displacement resolution of ~0.1 nm. Tests are performed inside the nanoindenter's thermally insulated environmental chamber at room temperature of 25 ± 0.5 ºC and relative humidity of 45 ± 2% on pure polymer, and PNC specimens of various volume fractions. The mechanical properties of the epoxy resin are highly dependent on the rate of testing [15], therefore, in order to be able to compare the results obtained for the unreinforced epoxy matrix and the nanocomposites, the test's parameters were held constant. A complete description of standard nanoindentation techniques is given by Bhushan and Li [16, 17]. Multiple indentation tests were applied over the surface of each sample. The samples (~500 μm in height) were mounted on an aluminium stub and indented to ~34 μm. The unloading load-displacement curves are analyzed to determine hardness and modulus using the Oliver-Pharr theory [18] with the projected area imaged under SEM as seen in the examples in Figure 5.

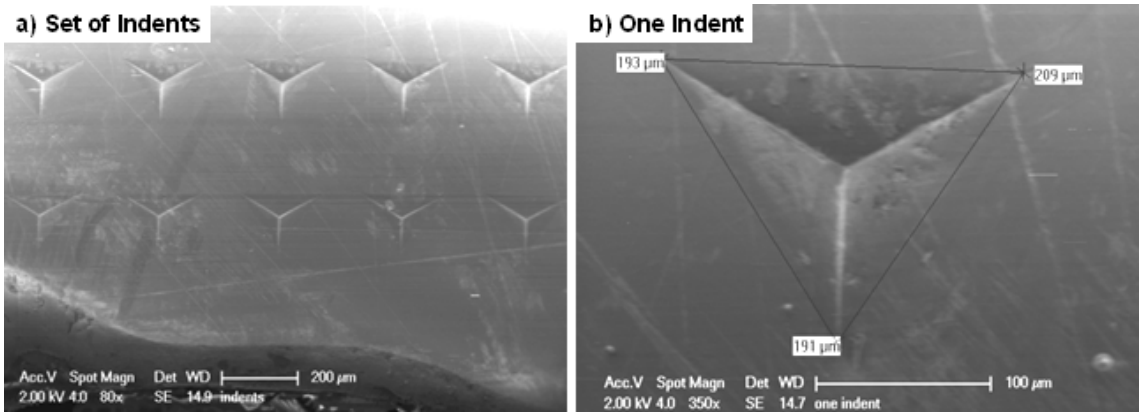

Figure 5. SEM imaging of nanoindented samples (VRM34, 6.6% V_f): (*left)* set of indents; (*right*) set of indents with measurements used to calculate indentation area. Scale bars are 200 μm and 100 μm, respectively.

D. Electrical Resistance Testing

DC resistance along the CNT axis is measured for the PNC specimens of various volume fractions. Aluminum plates (1 mm thick) are used as electrodes for the multimeter measurements, and the contact force on the plates is varied with a micrometer to ensure that good contact is made between the plates and the specimen. As the force on the plates from the micrometer increases, resistance decreases to a steady-state value at displacements approaching 50-100 microns. Sample dimensions are then used to calculate resistivity. The PNC sample dimensions were 300-600 μm high, and 1-4 mm wide.

III. Results and Discussion

Results are presented here for fabrication, mechanical, and electrical testing of the aligned-CNT PNCs. VRM34 resin was studied most extensively including modulus, hardness, and resistivity testing at various volume fractions and is the focus of the discussion herein.

A. Fabrication and Characterization

As discussed previously, in contrast to the lack of work on aligned-CNT PNCs, there is an extensive literature on non-ideal morphologies, centered on discontinuous, unaligned-CNTs at low V_f in polymer matrices. Three recent reviews survey the extant work on nanocomposites and identify the challenges [19-21]. The nanocomposite reviews are consistent with earlier literature (including other, older reviews [22-24]) and indicate that the PNCs studied here closely approximate the ideal morphology that has not been studied experimentally. Others have obtained high volume fraction aligned-CNT forests (dry) using solvent-induced densification of CNT forests [25,26]. In that method, a solvent is introduced and the capillary action from solvent evaporation densifies the CNT forests. This chemical densification method has not been reported for making nanocomposites, and our work indicates that it is not feasible to make well-controlled PNCs using chemical densification because of the cells formed in the forest when it is densified in this way. Mechanical densification is more controlled, allowing volume fraction to be continuously varied, and it can be managed so that cells (voids in a composite) are not formed over mm-scale dimensions.

It is difficult to image the CNTs inside the polymer using SEM. The smooth and insulating nature of the epoxy makes SEM visualization extremely difficult as has been found by numerous researchers. Improved SEM utilizing fracture surfaces, and TEM imaging (prepared with focused-ion-beam machining) of samples fabricated with an improved process have confirmed both CNT alignment and volume fraction within the PNCs [27]. An observed trend is that matrix-rich regions can form in the CNT forest during wetting. This is hypothesized to be a result of the contraction of the forest when the polymer first enters the CNT forest, contracting it somewhat, that is resisted at the top of the CNT forest because it is attached to the z-stage. At higher volume fractions, the matrix-rich regions diminish (see example trend in Figure 6). In the refined process recently developed, matrix-rich regions have been effectively eliminated by allowing the CNT forest to be wet by polymers while unattached to a z-stage and/or under slight mechanical compression.

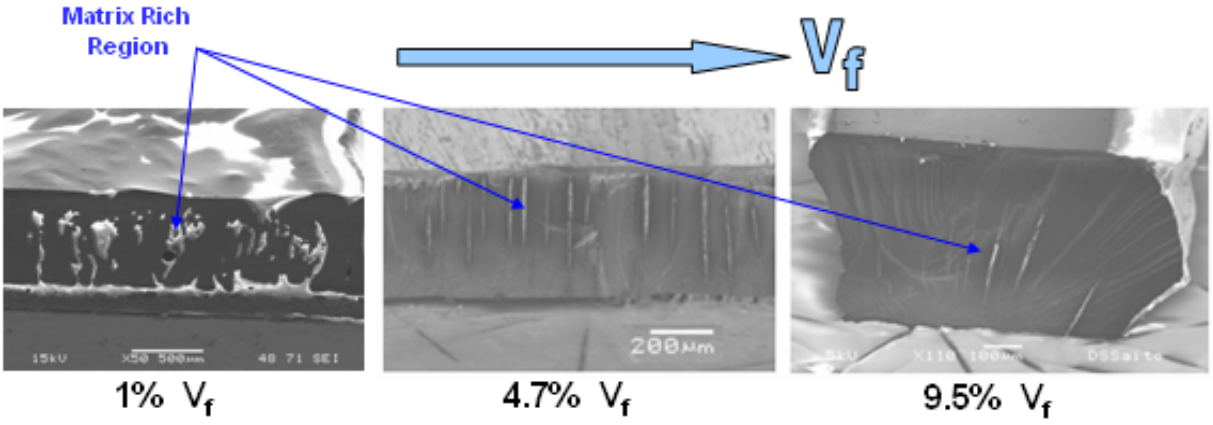

Figure 6. SEM images of a uniaxially-densified aligned-CNT PNC (VRM34 epoxy) at several V_f's. Scale bars are 500 μm, 200 μm, and 100 μm, respectively.

All epoxies in Table 1 were found to wet, via capillary action, the entire height (0.5 – 1 mm) of the CNT forests to form PNCs, even at high volume fraction (~20%) for the aerospace-grade epoxies. This result was somewhat surprising because at 20% V_f of CNTs, the inter-CNT spacing is on average 20-30 nm. This spacing is on the order of polymer chain characteristic lengths and is therefore in the range (10-100 nm [28]) where the polymer should be affected significantly by the presence of the CNTs. In an effort to explore morphology (packing, crystallization) changes of the polymer due to the small inter-CNT spacing, X-ray scattering studies were undertaken on a small set of polymers to explore any differences between the neat resin and the resin cured in the presence of the aligned-CNTs. X-ray scattering can provide information about the alignment and distribution of CNTs [29] and can also be

used in wide-angle mode (WAXS) to discern polymer morphology characteristics. It is beyond the scope of this paper to discuss the details of the WAXS theory and interpretation. However, the interpretation of the initial data is helpful to understand the degree to which CNTs are potentially affecting the structure (morphology) and therefore the properties of the polymer in the aligned-CNT PNC. VRM34 and RTM6 were studied in neat form and as PNCs at 4%, 1%, and 2% V_f via WAXS. Analysis of these results indicates that there is no evidence of polymer morphology change due to the presence of the CNTs [27]. This is a preliminary result, and recommendations to expand upon these findings are given in the Conclusions section.

B. Nanoindentation

Nanoindentation is used to extract hardness and also modulus information from VRM34 aligned-CNT PNCs at four CNT volume fractions (0%, 6.6%, 14.6%, and 16.6%). The nanoindentation procedures are as given above, and for each specimen at least 8 indents are performed to obtain averages. An example set of raw loading curves is given in Figure 7. A general trend that is observed is that higher CNT volume fractions generated less scatter in the reduced data, perhaps indicating that higher volume fraction samples displayed less effect of the CNT/polymer heterogeneity than at low volume fractions. A noted issue with nanoindentation of aligned-CNT PNCs into the ends of the CNTs is the likely spreading of the CNTs by the sharp indenter. Compression testing, either nanocompression or microcompression, should be explored in parallel with nanoindentation to study this effect.

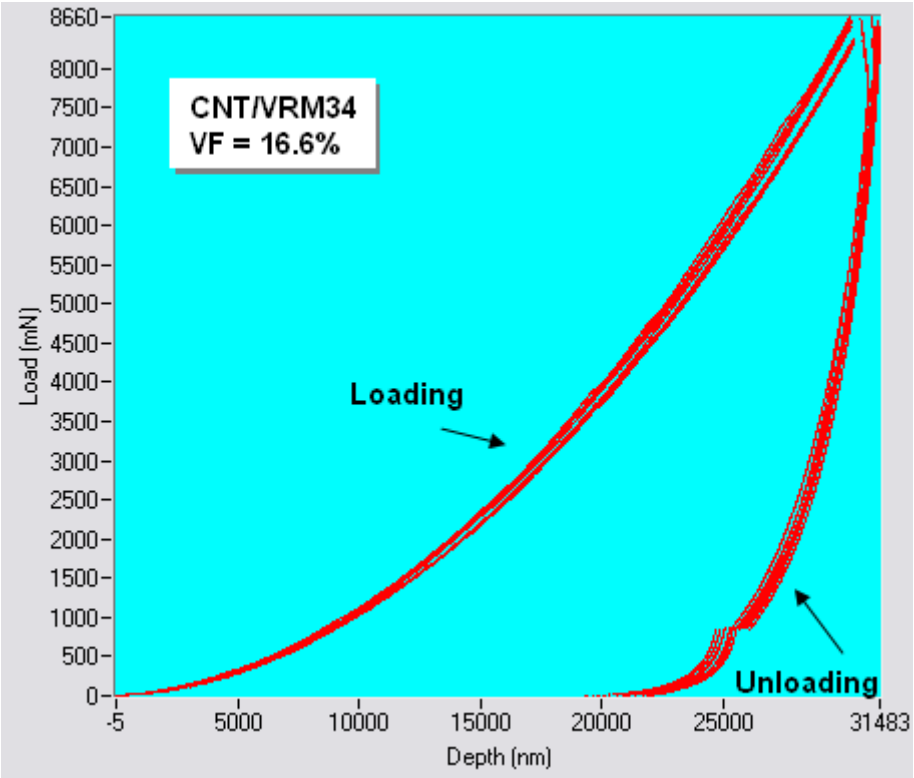

Figure 7. Nanoindentation loading curves for CNT/VRM34 aligned-CNT PNC.

Indentation and nanoindentation are generally accepted approaches for determining hardness (H) of a material. Hardness is obtained using the straightforward Vickers Hardness reduction involving the applied maximum force and the measured area of indentation (see Figure 5). Hardness is plotted vs. volume fraction in Figure 8, and there is no clear trend. The datapoint at 6.6% V_f has a lower hardness than even the pure resin. This CNT forest was *uniaxially* densified whereas the higher V_f forests were *biaxially* densified, so the results for hardness and also reduced modulus should be considered with this in mind. Modulus is obtained using the Oliver-Pharr theory and the unloading portion of the nanoindentation curve to obtain the reduced modulus (E_r). The reduced modulus is related to the specimen modulus through:

$$\frac{1}{E_r} = \frac{1-\nu^2}{E} + \frac{1-\nu_i^2}{E_i} \quad (1)$$

where E is the modulus of the sample, ν is the Poisson's ratio normal to loading of the sample, E_i is the indenter modulus, and ν_i is the indenter Poisson's ration normal to loading. The indenter is diamond with E_i = 1141 GPa and ν_i = 0.07, ν is taken as 0.3 due to the matrix (polymer) dominated response in this direction. The specimen Poisson's ratio would be expected to change as a function of V_f, but that effect is not considered in the data reduction herein. The specimen modulus is plotted vs. V_f in Figure 8. There is an increasing trend of modulus with V_f, although the datapoint at V_f = 6.6% needs to be discounted due to the uniaxial densification issue noted earlier. These initial results demonstrate some promise of nanoindentation to measure the hardness and modulus of aligned-CNT reinforced PNCs, but clearly more work is required due to the small available dataset. The modulus is noted to increase substantially due to the addition of the aligned-CNTs, increasing from ~5 GPa to nearly 15 GPa at 17% V_f. Note that the neat resin modulus compares favorably to the manufacturer stated flexural modulus of 4.9 GPa.

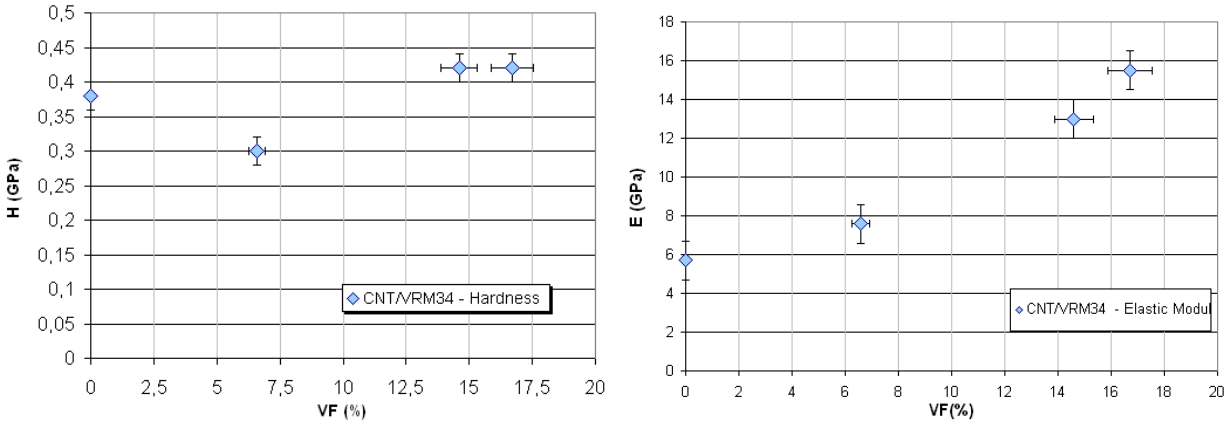

Figure 8. Hardness (H) and modulus (E) from nanoindentation testing of aligned-CNT PNCs using VRM34 epoxy as a function of volume fraction.

C. Electrical Resistance

Resistance of aligned-CNT PNCs is measured following the procedures described above, and then reduced to resistivity (ρ) using the specimen dimensions. A detailed investigation was carried out for the VRM34 resin over a range of V_f's up to ~9% (*uniaxially* densified), and the results are presented in Figure 9. It is expected that the PNCs should be conducting (due to the conducting nature of the MWCNTs because the CNTs are continuous from top to bottom in the conduction path. There is a clear trend of significantly decreased resistivity due to the CNTs, with the epoxy (0% V_f not plotted so as to visualize the conductive data) resistance registering as an open circuit (highly insulating) on the multimeter. Conductivity increase due to the presence of unaligned-CNTs in polymers is well-documented [30], but the authors are only aware of one study with aligned-CNT PNC electrical resistivity data [31]. In that study, the authors fabricated PNCs with polydimethylsiloxane (PDMS), a viscoelastic polymer, and observed a trend similar to that in Figure 8. Future work with the aligned-CNT PNCs will focus on comparing transport properties (electrical and thermal) along the CNT axis and transverse to it, where significant anisotropy is expected. Nano-engineered composites (see Figure 1) have demonstrated significantly enhanced conductivity due to the presence of aligned-CNTs grown on the surface of fibers in both DC and AC electrical testing [31-34]. Significant modeling needs to be undertaken to bridge the understanding of CNT electrical transport behavior to nano-engineered composite effective properties, likely through the study and modeling of aligned-CNT PNC RVEs (see Figure 1).

IV. Conclusions & Recommendations

Mechanical densification to achieve effective wetting and alignment of high-volume fraction CNT/polymer nanocomposites has been presented. Such composites are of interest for various applications and comprise representative volume elements of three-dimensional CNT-reinforced nano-engineered composites under development. Ultra-high volume fraction aligned and continuous-CNT nanocomposites may have tremendous

potential for numerous applications. Nanocomposites at the scale currently demonstrated are of interest in applications where good electrical and/or thermal conductivities are required. The mechanical densification method presented here is an early version, and has been recently improved. As presented in the Results section, wetting is effective to ~20% CNT volume fraction for the unmodified (no solvents added) aerospace-grade thermosets. Preliminary characterization via wide-angle X-ray scattering for three thermosets indicates no morphology change due the presence of the aligned-CNTs. Mechanical properties of these nanocomposites (their Young´s modulus in particular) increase with higher V_f's of CNTs. Conductivity enhancement of several orders of magnitude is noted when CNTs are introduced into the polymer with conductivity increasing as a function of CNT V_f.

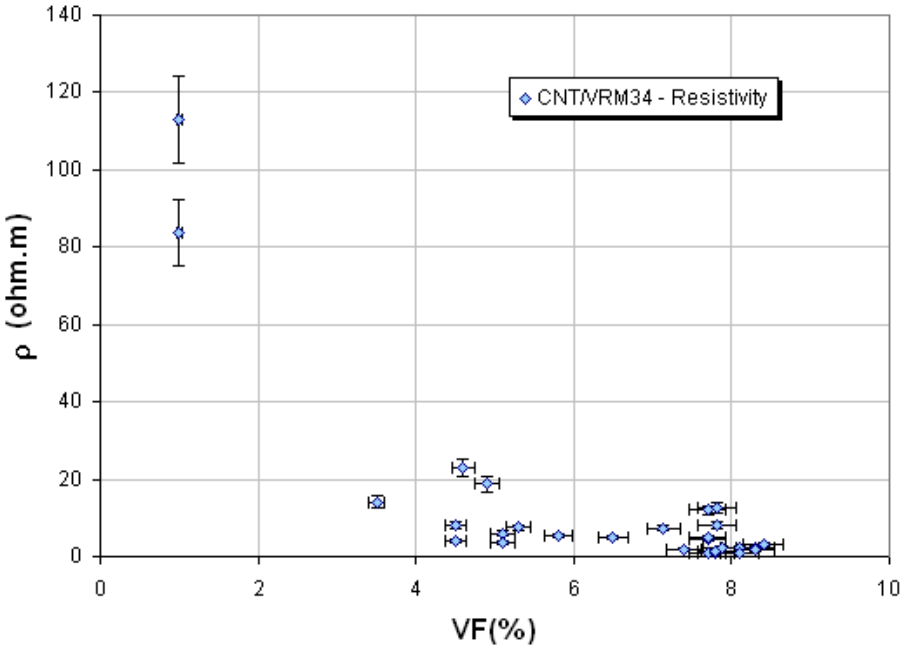

Figure 9. Resistivity trend with V_f for aligned-CNT PNC (VRM34 epoxy) along the CNT axis.

Future research will focus on finding an upper limit of CNT volume fraction that can be wet by a given polymer and correlated to governing physical properties such as contact angle and viscosity. The preliminary results presented in this paper show clear trends with volume fraction, but further multifunctional (*i.e.,* mechanical, electrical, thermal) tests are needed on improved specimens to fully characterize the high-V_f PNC materials, particularly fracture and strength properties for structural applications. The mm-scale nanocomposite specimens should provide an effective experimental platform for studying topics such as CNT functionalization, polymer modification, other processing effects such as microwave bonding, non-isotropic physical behavior (such as stiffness along the CNT axes vs. transverse to it), the effects of CNT-CNT interactions (touching) on transport properties, and the effects of very closely spaced CNTs on morphology changes of various polymer matrices including thermoplastics.

Acknowledgments

This work was supported by Airbus S.A.S., Boeing, Embraer, Lockheed Martin, Saab AB, Spirit AeroSystems, and Textron Inc. through MIT's Nano-Engineered Composite aerospace STructures (NECST) Consortium. The authors gratefully acknowledge Namiko Yamamoto (MIT) and Hulya Cebeci (MIT) for valuable input into this manuscript. The authors thank John Kane and the entire Technology Laboratory for Advanced Materials and Structures (TELAMS) at MIT for technical support, Patrick Boisvert at the Center for Materials Science and Engineering at MIT for imaging assistance, Alan Schartzmann at the Nanomechanical Technology Laboratory (NanoLab) at MIT, and Hexcel Corp. for providing resin used in this work.

References

[1] S. Iijima. "Helicoidal microtubes of graphitic carbon." *Nature*, vol. 354, pp. 56-58, 1991.

[2] A. Oberlin, M. Endo and T. Koyama. "Filamentous Growth of Carbon Through Benzene Decomposition." *Journal of Crystal Growth*, vol. 32, pp. 335-349, 1976.

[3] E. J. Garcia, J. Hart, B. L. Wardle, and A. Slocum. "Composite Materials Reinforced with Long CNTs Grown on the Surface of Fibers," in *Proc. AIAA-2006-1854, 47th AIAA Structures, Dynamics, and Materials Conference*, 2006.

[4] E. J. Garcia, J. Hart, B. L. Wardle, and A. Slocum. "Aligned Carbon Nanotube Reinforcement of Ply Interfaces in Woven Composites," in *Proc. AIAA-2007-2037, 48th AIAA Structures, Dynamics, and Materials Conference*, 2007.

[5] E. J. Garcia, J. Hart, B. L. Wardle, A. Slocum, and D.J. Shim. "Aligned Carbon Nanotube Reinforcement of Graphite/epoxy Ply Interfaces," in *Proc. 16th International Conference on Composite Materials (ICCM)*, 2007.

[6] E. J. Garcia, J. Hart, B. L. Wardle, and A. Slocum. "Fabrication and Nanocompression Testing of Aligned CNT/Polymer Nanocomposites." *Advanced Materials*, vol. 19, pp. 2151-2156, 2007.

[7] O. Probst, E. M. Moore, D. E. Resasco, B. P. Grady. "Nucleation of polyvinyl alcohol crystallization by single-walled carbon nanotubes." *Polymer*, vol. 45 (13), pp. 4437–43, 2004.

[8] F. Dalmas, L. Chazeau, C. Gauthier, K. Masenelli-Varlot, R. Dendievel, J. Y. Cavaillé, et al. "Multiwalled carbon nanotube/polymer nanocomposites: processing and properties." *J Polym Sci Part B: Poly Phys*, vol. 43 (10), pp. 1186–97, 2005.

[9] A. J. Hart, and A. Slocum. "Nucleation, Rapid Growth, and Mechanical Stability of Millimeter-Scale Aligned Carbon Nanotube Structures Growth by Thermal CVD at Atmospheric Pressure." *Journal of Physical Chemistry B*, vol. 110 (16), pp. 8250-8257, 2006.

[10] E. J. Garcia, J. Hart, and B. L. Wardle. "Long Carbon Nanotubes Grown on the Surface of Fibers for Hybrid Composites." AIAA Journal, vol. 46 (6), pp. 1405-1412, 2008.

[11] E. J. Garcia, J. Hart, B. L. Wardle, and A. Slocum. "Fabrication of composite microstructures by capillarity-driven wetting of aligned carbon nanotubes with polymers." *Nanotechnology,* vol. 18, pp. 165602-165612, 2007.

[12] Bello, D., Wardle, B.L, Ahn, K., Yamamoto, N., Garcia, E.J., Hart, A.J., and M.J. Ellenbecker, "Exposure to Nanoscale Particles and Fibers During Fabrication and Machining of Hybrid CNT Advanced Composites." *J. Nanoparticle Research*, vol. 11 (1), pp. 231-249, 2009.

[13] D. Bello, A. J. Hart, K. Ahn, M. Hallock, N. Yamamoto, E. J. Garcia, M. J. Ellenbecker, B. L. Wardle. "Exposure to nanoscale particles during CVD growth of CNTs and their subsequent handling." *Carbon*, Vol. 46, pp. 974-978, 2008.

[14] http://www.micromaterials.co.uk/

[15] A. Gilat, R. K. Goldberg, and G. D. Roberts. "Strain Rate Sensitivity of Epoxy Resin in Tensile and Shear Loading" in NASA/TM-2005-213595, 2005.

[16] X. Li and B. Bhushan. "A Review of Nanoindentation Continuous Stiffness Measurement Techniques and Its Applications." *Mater. Characterization*, vol. 48, pp. 11-36, 2002.

[17] B. Bhushan and X. Li. "Nanomechnical Characterization of Solid Surfaces and Thin Films." *Int. Mater. Rev.* vol. 48, pp. 125-164, 2003.

[18] W. C. Oliver and G. M. Pharr. "An improved Technique for Determining Hardness and Elastic Modulus Using Load and Displacement Sensing Indentation Experiments." *J. of Mater. Res.*, vol. 7, pp. 1564-1583, 1992.

[19] P. M. Ajayan and J. M. Tour. "Material Science: Nanotube Composites." *Nature* vol. 447, pp. 1066-1068, 2007.

[20] K. Schulte and A. H. Windle. "Editorial." *Composites Science & Technology*, vol. 67, pp. 777, 2007.

[21] A. H. Windle. "Personal View." *Composites Science & Technology*, vol. 67, pp. 929-930, 2007.

[22] J. N. Coleman, U. Khan, W. J. Blau, Y. K. Gun'ko. "Small but strong: A review of the mechanical properties of carbon nanotube - polymer composites." *Carbon*, vol. 44, pp. 1624-1652, 2006.

[23] E. T. Thostenson, C. Li C., and T. W. Chou. "Nanocomposites in Context." *Composites Science and Technology*, vol. 65, pp. 491–516, 2005.

[24] E. T. Thostenson, Z. Ren, and T. W. Chou. "Advances in the Science and Technology of Carbon Nanotubes and Their Composites: A Review." *Composites Science and Technology*, vol. 61, pp. 1899-1912, 2001.

[25] N. Chakrapani, B. Wei, A. Carrillo, P. M. Ajayan, and R. S. Kane. "Capillarity-driven assembly of two-dimensional cellular carbon nanotube foams," in *Proc. of the National Academy of Science*, vol. 101 (12), pp. 4009-4012, 2004.

[26] D. N. Futaba, K. Hata, et al. "Shape-engineerable and highly densely packed SWNTs and their application as supercapacitor electrodes." *Nature Materials*, vol. 5, pp. 987-994, 2006.

[27] B. L. Wardle, D. S. Saito, E. J. Garcia, A. J. Hart, and R. Guzman deVilloria, "Fabrication and Characterization of Ultra-High Volume Fraction Aligned Carbon-Nanotube-Polymer Composites." *Advanced Materials*, vol. 20 (14), pp. 2655-2796, 2008.

[28] P. M. Ajayan,, P. Braun, and L. Schadler. in *Nanocomposite Science and Technology*, Ed. W. Wiley-VCH. 2003.

[29] B. N. Wang, R. D. Bennett, E. Verploegen, A. J. Hart, R. E. Cohen, "Quantitative Characterization of the Morphology of Multi-Wall Carbon Nanotube Films by Small-Angle X-ray Scattering." *J. Physical Chemistry C*, vol. 111(16), pp. 5859-5865, 2007.

[30] W. Bauhofer, J. Z. Kovacs. "A review and analysis of electrical percolation in carbon nanotube polymer composites." *Composites Science and Technology*, vol. 69 (10), pp. 1486-1498, 2009

[31] L. Ci, J. Suhr, V. Pushparaj, X. Zhang, and P. M. Ajayan. "Continuous Carbon Nanotube Reinforced Composites." *Nano Lett.*, vol. 8 (9), pp. 2762-2766, 2008

[32] E. J. Garcia, B. L. Wardle, A. J. Hart, and N. Yamamoto, "Fabrication and Multifunctional Properties of a Hybrid Laminate with Aligned Carbon Nanotubes Grown In Situ." *Composites Science & Technology*, vol. 68 (9), pp. 2034-2041, 2008.

[33] N. Yamamoto, and B.L. Wardle, "Thermal and Electrical Properties of Hybrid Woven Composites Reinforced with Aligned Carbon Nantoubes," in *Proc. 49th AIAA Structures, Dynamics, and Materials Conference*, 2008, AIAA-2008-1857.

[34] E. J. Garcia, J. Hart, B. L. Wardle, A. Slocum, and R. Guzman de Villoria, "Aligned Carbon Nanotube Reinforcement of Advanced Composite Ply Interfaces," *49th AIAA Structures, Dynamics, and Materials Conference*, 2008, AIAA-2008-1768.